Published in final edited form as:
Nat Neurosci. 2007 October ; 10(10): 1260–1267. doi:10.1038/nn1966.

Stargazin attenuates intracellular polyamine block of calcium-permeable AMPARs

David Soto, **Ian D. Coombs**, **Leah Kelly**, **Mark Farrant**[†], and **Stuart G. Cull-Candy**[†]
Department of Pharmacology, University College London Gower Street, London WC1E 6BT UK

Abstract

Endogenous polyamines profoundly affect the activity of various ion channels, including that of calcium-permeable AMPA-type glutamate receptors (CP-AMPARs). Here we show that stargazin, a transmembrane AMPAR regulatory protein (TARP) known to influence transport, gating and desensitization of AMPARs, greatly reduces block of CP-AMPARs by intracellular polyamines. By decreasing CP-AMPAR affinity for cytoplasmic polyamines, stargazin enhances the charge transfer following single glutamate applications and eliminates the frequency-dependent facilitation seen with repeated applications. In cerebellar stellate cells, which express both synaptic CP-AMPARs and stargazin, we found that the rectification and unitary conductance of channels underlying excitatory postsynaptic currents were matched by those of recombinant AMPARs only when the latter were associated with stargazin. Taken together, our observations establish modulatory actions of stargazin specific to CP-AMPARs, and suggest that during synaptic transmission the activity of such receptors, and thus calcium influx, is fundamentally changed by TARPs.

INTRODUCTION

AMPA type glutamate receptors mediate most fast excitatory synaptic transmission in the brain. The AMPAR subunits (GluR1-GluR4) form tetrameric assemblies with properties that depend crucially on their constituent subunits – in particular, the presence of GluR2. This subunit is modified at its Q/R site in the pore-lining region by posttranscriptional RNA editing1. Unlike other AMPARs, those lacking the edited GluR2 subunit are permeable to Ca^{2+} ions2, possess a high single-channel conductance3,4, and are subject to a block by endogenous intracellular polyamines that confers profound rectification on the responses5-7 and influences frequency-dependent facilitation at synapses expressing these receptors8,9. CP-AMPARs have also been implicated in the induction of NMDAR-dependent long-term potentiation10 (but see also ref. 11) and in various neurological conditions4,12-15, and are themselves subject to dynamic regulation15-19.

AMPARs are modulated by interaction with stargazin, a TARP that is crucial for their surface expression20-22, synaptic targeting and stabilization23, and recycling24.In addition, stargazin interacts with AMPARs to slow channel deactivation and desensitization25-29 and to increase the rate of channel opening26. Previous studies, however, have not revealed functional effects of stargazin on the characteristic rectification of CP-AMPARs26,30.

Here we describe how stargazin regulates the functional properties of recombinant homomeric CP-AMPARs (comprising GluR1, GluR3 or GluR4) by influencing block by polyamines and enhancing Ca^{2+} transfer. We show that stargazin reduces the sensitivity of

[†]Authors for correspondence: Stuart Cull-Candy, Tel. +44(0)20 7679 3766, Fax. +44(0)20 7679 7298, e-mail: s.cull-candy@ucl.ac.uk Mark Farrant, Tel. +44(0)20 7679 4121, Fax. +44(0)20 7679 7298, e-mail: m.farrant@ucl.ac.uk.

Europe PMC Funders Author Manuscripts

CP-AMPARs to polyamine block at both positive and negative membrane potentials. This effect, which is not accompanied by modification in the permeability of channels to Ca^{2+} ions, is associated with a marked increase in single-channel conductance. These altered channel properties, combined with a slowed channel deactivation time, are expected to enhance the macroscopic conductance, to increase Ca^{2+} influx, and to alter frequency-dependent facilitation.

To determine whether stargazin exerts a similar influence on the properties of native CP-AMPARs, we also examined synaptic currents in cerebellar stellate cells. These cells show strongly rectifying synaptic currents, indicative of the presence of GluR2-lacking AMPARs16,18,31, and are known to express stargazin32-34. We find that AMPARs underlying stellate cell excitatory postsynaptic currents (EPSCs) show rectification and single-channel properties that correspond well to those of recombinant AMPARs coexpressed with stargazin. Our results support the view that TARPs play an essential part in determining basic EPSC properties in neurons expressing CP-AMPARs.

RESULTS

Stargazin alters rectification of recombinant CP-AMPARs

To examine the effect of stargazin on CP-AMPARs, we recorded glutamate-evoked currents from recombinant receptors expressed in tsA201 cells (**Methods** and Supplementary Methods online), and measured the effect of stargazin on current-voltage (*I-V*) relationships obtained in response to rapid applications of glutamate (10 mM, 100 ms) to outside-out membrane patches (Fig. 1). The glutamate-evoked responses from homomeric AMPARs composed of GluR1 (Fig. 1a) or GluR4 (Fig. 1b) showed characteristic inwardly rectifying *I-V* plots due to block by intracellular polyamine (100 μM added spermine). In the presence of stargazin, rectification was markedly reduced, although not abolished, at both negative and positive potentials (Fig. 1a, b). Similar results were obtained for homomeric GluR3 (data not shown). **S**targazin greatly reduced rectification of glutamate-evoked currents from outside-out patches taken from cells expressing GluR4 (Fig. 1c). By contrast, Ca^{2+}-impermeable AMPARs (heteromeric GluR2/GluR4) generated linear *I-V* plots (Fig. 1d) that were unchanged by stargazin. The stargazin used in these experiments was tagged at the carboxy-terminus with enhanced green fluorescent protein (EGFP[20]), but identical effects were obtained with stargazin that lacked EGFP (data not shown).

Channel conductance, but not Ca^{2+} permeability is modified

The spermine sensitivity of AMPARs is determined by Q/R editing in the channel pore, which is also critical for their Ca^{2+} permeability. To determine whether the decrease in spermine sensitivity of GluR2-lacking (Ca^{2+}-permeable) AMPARs was accompanied by a change in their Ca^{2+} permeability, we compared the reversal potentials of glutamate-evoked currents in solutions containing low (1 mM) or high (30 mM) Ca^{2+} (Fig. 2). For receptors with high Ca^{2+} permeability, partial replacement of external Na^+ with Ca^{2+} should not change the reversal potential. Indeed, we found no shift with homomeric GluR4 AMPARs (Fig. 2a). We obtained similar results when GluR4 was coexpressed with stargazin (Fig. 2c), suggesting that the Ca^{2+} permeability of the channels was unaltered. From the reversal potentials, we estimated the relative Ca^{2+} permeability (P_{Ca}/P_{Na}) and obtained similar values for GluR4 (0.87) and GluR4 with stargazin (0.82). This values contrasted with those obtained for heteromeric GluR2/GluR4 AMPARs, which, as expected for Ca^{2+}-impermeable receptors, showed a large negative shift in reversal potential in high-Ca^{2+} (−1.1 ± 1.3 mV in Na^+ -rich solution, as compared with −57.8 ± 3.3 mV in Ca^{2+} -rich solution; n = 4, P_{Ca}/P_{Na} = 0.04).

Although stargazin did not modify Ca^{2+} permeability, it caused a significant increase in AMPAR single-channel conductance26. Non-stationary fluctuation analysis of responses evoked by 10mM glutamate yielded conductance estimates of 17.6 ± 2.7pS for homomeric GluR4 AMPARs (Fig. 2b), and 25.4 ± 2.0pS when GluR4 was expressed with stargazin (Fig. 2d; n=15 and 16 cells, respectively; P=0.013). By contrast, the maximum open probability of the channels ($P_{o,max}$) was unchanged (0.61 ± 0.05 versus 0.68 ± 0.04, P=0.336).

What are the overall effects of stargazin on charge transfer and Ca^{2+} influx through CP-AMPARs? As indicated above, stargazin increased the single-channel conductance of GluR4 by ~40% (Fig 2). For a 1ms application of glutamate, stargazin also slowed deactivation by ~140% (Fig. 3a). By plotting conductance against voltage35 it can be seen that stargazin induced a +33 mV shift in the voltage for half-maximal block by spermine (Fig. 3b). Consequently, in response to a brief pulse of glutamate at a typical neuronal resting potential of −60mV, the alleviation of spermine block by stargazin resulted in an additional increase in the macroscopic conductance of ~30%. Although the stargazin-induced change in single-channel conductance and kinetics may be similar for all AMPARs, the modulation of spermine action by stargazin is specific to Ca^{2+}-permeable receptors. Given the lack of change in Ca^{2+} permeability, this modulation would result in an additional increase in Ca^{2+} influx.

Stargazin reduces channel block by polyamines

We tested whether stargazin altered the time course of spermine open-channel block. Although the mechanism by which endogenous intracellular polyamines block CP-AMPARs is not fully understood, they seem to act as an open-channel blocker and to bind to closed-channel states8. Because the onset and recovery of AMPAR block by polyamines is rapid, we applied voltage steps in the presence of 1mM glutamate and 50 μM cyclothiazide to patches expressing GluR4 with and without stargazin (Fig. 4a-d).

Peak current responses to voltage steps were followed by clear relaxations in patches expressing GluR4 alone, as expected for open-channel block by spermine (Fig. 4a). These relaxations were greatly slowed when stargazin was coexpressed with GluR4 (Fig. 4b), suggesting that stargazin reduced sensitivity to spermine. The *I-V* relationships constructed for the peak responses showed relatively weak rectification, regardless of the presence of stargazin (Fig. 4a, b, bottom). This observation contrasted with that for steady-state currents, which yielded a markedly rectifying *I-V* plot only in the absence of stargazin (Fig. 4a versus b).

To examine recovery from spermine block, patches were stepped from a holding potential of +20mV to −80mV in −20 mV increments. The re-equilibration rates of the current (from blocked to unblocked state) were significantly faster with stargazin present (Fig. 4c,d). For GluR4 alone, the equilibration when stepping from +20 to −60mV was described by a double exponential (τ_f = 67±11 μs (67±9 %), τ_s = 339±101 μs; τ_w = 158±27 μs, n = 6), whereas for GluR4 plus stargazin only a single exponential was required (τ = 38±1μs, n = 4, P=0.007 versus τ_w of GluR4). These results indicate a markedly accelerated spermine unblock occurred in the presence of stargazin.

Stargazin alters frequency-dependent facilitation

We considered whether this change in polyamine block could have physiological consequences. Polyamines produce a closed-channel block that is voltage insensitive but relieved by cation influx, giving rise to an activity-dependent postsynaptic facilitation (or reduced depression) at physiologically relevant frequencies of activation8,36. To determine

whether stargazin altered this facilitation, we applied trains of glutamate pulses (1ms, 1mM, 14 Hz) to patches (Fig. 4e, f). We obtained modest facilitation with GluR4 alone (+12.2 ± 3.1%, *n*=16; Fig. 4e, g) but no facilitation when stargazin was present; instead, the currents showed clear depression (−8.2 ± 2.9%, *n*=9: Fig. 4f, g), consistent with incomplete recovery from desensitization at this frequency (which was also evident in the absence of spermine; data not shown).

Stargazin influences properties of synaptic CP-AMPARs

To assess whether spermine modulation of synaptically activated CP-AMPARs is likely to be altered by stargazin, we examined EPSCs in cerebellar stellate cells. These cells show rectifying EPSCs, indicative of the presence of GluR2-lacking AMPARs16, and also express stargazin32-34. We reasoned that, if stargazin is bound to synaptic CP-AMPARs, then it is likely to influence EPSC rectification and to increase the underlying single-channel conductance26.

Our experiments showed that rectification of these EPSCs was strongest in young rats, when AMPARs are likely to be homomeric GluR3 assemblies, and decreased during development, reflecting the expression of mainly heteromeric GluR2/3 assemblies37,38. Figure 5 shows families of parallel fibre-evoked EPSCs, recorded over a range of membrane voltages from stellate cells taken from rats at postnatal day 8 (P8), P18 and P28 (100 μM added spermine). Rectification (calculated as rectification index; **Methods**) was greatest at P8 (0.34 ± 0.03, n = 23) when the EPSCs are mediated almost completely by CP-AMPARs16. In cells from P18 and P28 rats the *I-V* relationships were less rectifying, as indicated by higher rectification index values (0.60 ± 0.04 and 0.48 ± 0.06, respectively; n = 19 and 8, $P<0.0001$ and $P=0.02$ versus P8, Mann-Whitney *U*-test). EPSC rectification was due to the blocking action of intracellular spermine: with a spermine-free intracellular solution, rectification was absent and the rectification index was consistent across all ages (mean 1.00 ± 0.01 (n = 6) at P8, 1.00 ± 0.01 (n = 4) at P18 and 1.00 ± 0.07 (n = 4) at P28).

We applied peak-scaled non-stationary fluctuation analysis (psNSFA; **Methods**) to spontaneous EPSCs to estimate the single-channel conductance of synaptic AMPARs39. Single-channel conductance was greatest in young rats and decreased with age (Fig. 5b; n = 36, $P=0.022$, Spearman rank-order correlation), consistent with the insertion of GluR2-containing AMPARs at older synapses3. The rectification and single-channel conductance of synaptic AMPARs are expected to reflect not only their subunit composition, but also the presence of stargazin. Comparison of stellate cell data with conductance and rectification measures obtained from GluR3 and GluR2/GluR3 recombinant AMPARs (Fig. 5c) showed that the properties of the native channels were matched only by those of recombinant receptors coexpressed with stargazin. Of note, all EPSCs showed a rectification index greater than 0.15. When GluR3 was expressed without stargazin, by contrast, it gave average rectification index values of 0.01 ± 0.01 (n = 8). In fact, 75% of patches expressing GluR3 alone showed no outward current at +40mV (rectification index 0). When GluR3 was expressed with stargazin, the rectification index (0.13 ± 0.03, n = 8, $P=0.0013$) moved closer to that shown by EPSCs mediated predominantly by CP-AMPARs.

Mechanism of altered channel block

Although the experiments shown in Figure 4a,b suggest that stargazin modulates the *I-V* relationship of CP-AMPARs by altering sensitivity to polyamines, such a result could arise from a change in intrinsic properties of channel gating. To test this possibility, we examined the *I-V* relationship of GluR4 AMPARs with and without stargazin in the absence of any intracellular polyamines. Endogenous polyamines were chelated by inclusion of 20 mM Na_2ATP in the internal solution, and experiments were performed >10 min after patch

excision. There was identical outward rectification in the two conditions (Fig. 6). Thus, we conclude that the effects of stargazin on GluR4 AMPAR inward rectification in the presence of polyamines are mediated solely by modulation of polyamine block.

We considered how the binding of stargazin to CP-AMPAR channels could produce a change in spermine block. To determine whether the affinity of the channels for spermine was changed in the presence of stargazin, we examined *I-V* relationships obtained with different concentrations of added spermine (1-500 μM; Fig. 7a, b). Plots of normalized conductance against free spermine concentration (**Methods**) were used to estimate the apparent affinity of the channels for spermine at various membrane voltages. The half-maximal inhibitory concentration (IC_{50}) values decreased as the patch was depolarized, both in the presence and absence of stargazin (Fig. 7c,d; for clarity, only negative voltages are shown). For AMPARs coexpressed with stargazin, the IC_{50} was markedly reduced at both negative and positive potentials (Fig. 7e); extrapolated linear fits of the data indicated a 22-fold decrease in apparent affinity at 0 mV in the presence of stargazin. The effect of stargazin appeared broadly similar at both negative and positive membrane potentials, suggesting that its action could be adequately explained by a change in spermine affinity. It was not possible to quantify separately the contribution of any change in spermine permeation. Specifically, the pronounced attenuation of spermine block meant that, from our kinetic data (Fig. 4b), we were unable to derive the constraints necessary to enable resolution of all parameters of a Woodhull-type model for a weakly permeating blocker35.

We also considered whether modulation by stargazin similarly affected block by spermidine, another endogenous polyamine. Spermine and spermidine differ both in their chain length (ten and seven CH_2 groups, respectively) and the number of positively charged groups (four and three NH_2 groups, respectively). Comparison of the GluR4 *I-V* relationships (Figure 8a,b) shows that stargazin had a similar influence on the action of both polyamines (100 μM added). To estimate the effect of stargazin on polyamine affinity, we plotted normalized conductance against voltage (Fig. 8c,d; corrected for the outward rectification seen in the absence of polyamines, Fig. 6). The data at negative potentials (describing the onset of polyamine block) were fitted to a Woodhull model for an impermeable blocker according to $K_d = K_{d(0)} \exp(-V_m z\delta F/RT)$, where $K_{d(0)}$ is the apparent dissociation constant at 0 mV, z is the valence of the polyamine, V_m is the membrane voltage, δ is the fraction of the membrane electric field experienced by the polyamine, and R, T and F have their conventional meanings8,35. For both polyamines, stargazin produced a roughly tenfold increase in $K_{d(0)}$, from 0.49 to 4.54 μM with spermine, and from 0.98 to 9.1 μM with spermidine. By contrast, δ was essentially unchanged for both polyamines ($z\delta$ = 0.40 versus 0.36, $z\delta$ = 1.6 versus 1.44 with spermine; $z\delta$ = 0.6 versus 0.55, $z\delta$ = 1.8 versus 1.65 with spermidine). The fact that the values of $K_{d(0)}$ for spermine differ from the extrapolated values of IC_{50} at 0 mV (Fig. 7) is not unexpected, given that the Woodhull model is not formally applicable in this case35. Nevertheless, it is clear that stargazin produced a comparable shift in the affinity of GluR4 receptors for both spermine and spermidine.

DISCUSSION

We have shown that channel properties of all three homomeric CP-AMPAR subtypes (comprising GluR1, GluR3 and GluR4) are modified by coassembly with the membrane spanning protein stargazin. In particular, we found that channel block by intracellular polyamines is markedly reduced at all potentials. AMPARs are considered to be physically associated with TARPs and are anchored by them in the postsynaptic membrane23,24. Our experiments on synaptic CP-AMPARs suggest that the associated TARP is crucial in determining the sensitivity of the native channels to endogenous cytoplasmic polyamines.

Stargazin enhances charge transfer by modifying polyamine block

In the presence of stargazin, we found that block of recombinant CP-AMPARs by intracellular polyamines is reduced, unblock of channels is accelerated, and single-channel conductance is increased. Because these modifications are not associated with a reduction in maximum open probability, we estimate that the total charge transfer will be at least doubled. In addition, because Ca^{2+} permeability of the channels is unaltered, there will be a corresponding increase in Ca^{2+} entry. These changes are likely to influence several key aspects of transmission at synapses with CP-AMPARs (see below).

We considered possible ways in which the presence of stargazin might influence the mechanism of spermine block. The more than 20-fold shift in spermine IC_{50} at both negative and positive potentials suggests that a simple reduction in the affinity of the channel for polyamine molecules can account for the change in the *I-V* relationship; this possibility does not exclude involvement of other factors. Our data concerning the block produced by spermine and spermidine is consistent with the idea that, as previously found for kainate receptors5,35, both polyamines can permeate CP-AMPAR channels. In preliminary experiments, we have found that other TARPs (γ-4 and γ-8), which show subtle differences in structure from stargazin, have a qualitatively similar effect on polyamine block (data not shown).

Are native postsynaptic receptors similarly affected by stargazin?

Stargazin and other members of the TARP family interact with all four AMPAR subunits26,29, and are involved in the surface expression and synaptic localization of AMPARs20,21,23. Our experiments on cerebellar stellate cells, which express both Ca^{2+}-permeable and -impermeable synaptic AMPARs16,31, suggest that both AMPAR subtypes show properties expected of TARP-associated receptors.

The conductance and rectification properties of AMPARs underlying the EPSCs in stellate cells corresponded well to the properties of recombinant AMPAR subunits only when the latter subunits were coexpressed with stargazin. In young rats, stellate cell EPSCs are predominantly mediated by CP-AMPARs (most probably homomeric GluR3; refs. 16,31,38) and there is a gradual switch to Ca^{2+}-impermeable AMPARs (GluR2-GluR3; refs. 16,31, 38). Thus, during development, the synaptic AMPARs show a continuum of conductance and rectification properties, reflecting a gradual developmental increase in the proportion of Ca^{2+}-impermeable receptors. In recordings from recombinant GluR3 and GluR2/GluR3 AMPARs, we found that this continuum was poorly followed by receptors lacking stargazin but was matched well by those containing this TARP. In keeping with this finding, stellate cells are known to express stargazin32-34. We do not, of course, exclude the possibility that other TARPs also contribute to the synaptic channels in stellate cells. Our observations strongly support the view that postsynaptic CP-AMPARs are modified by TARPs *in situ*, and that this modification enhances charge transfer and thus Ca^{2+} entry.

Our data are consistent with the view that polyamines block the closed state, in addition to the open state of the CP-AMPAR8,36, because stargazin modulation was sufficient to alter polyamine-dependent facilitation. In fact, our data suggest that the facilitation associated with postsynaptic CP-AMPARs might be less profound than was previously thought9. In addition, the enhancement in Ca^{2+} influx due to stargazin is likely to be particularly important in interneurons such as cerebellar stellate cells, where increased postsynaptic Ca^{2+} mediates both synaptic targeting of Ca^{2+}-impermeable GluR2-containing AMPARs15,16,18 and activation of intracellular signaling cascades associated with the production and release of endocannabinoids 40,41.

Compelling evidence indicates that changes in the intraneuronal concentration of polyamines can dynamically modulate the CP-AMPARs underlying some EPSCs, both during development[42] and after sustained activity[43]. Whether modulation of polyamine block also occurs as a result of dynamic changes in the binding/unbinding of stargazin to AMPARs, or indeed whether 'TARP-less' AMPARs exist either synaptic or extrasynaptic sites, is at present unclear[21,25]. TARPs are differentially expressed with respect to brain region and ontogeny, and it seems likely that different TARPs may vary markedly in their influence on properties of individual CP-AMPAR subtypes[29]. If so, the level, species or stoichiometry of TARP expressed might directly determine sensitivity to polyamine block at particular synapses. It is clear that the relative abundance and targeting of GluR2 can shape EPSC properties and control Ca^{2+} permeability at central synapses [2,16,44-46]. Our results suggest that stargazin also has a decisive role in determining the properties CP-AMPAR EPSCs.

Methods

Recombinant receptors

tsA201 cells were grown according to standard protocols and transfected with DNA encoding AMPAR subunit and stargazin-EGFP by using Lipofectamine 2000 (Invitrogen;see Supplementary Methods).

Electrophysiology

Macroscopic currents were recorded at room temperature (22-24 °C) from outside-out patches excised from EGFP-positive cells (see Supplementary Methods). The 'external' solution contained (in mM): 145 NaCl, 2.5 KCl, 1 $CaCl_2$, 1 $MgCl_2$, 10 glucose and 10 HEPES (pH 7.3 with NaOH). For agonist solutions, 1 or 10mM glutamate and, where indicated 50 μM cyclothizaide (Tocris Bioscience) were added. The 'internal' (pipette) solution contained: (in mM) 145 CsCl, 2.5 NaCl, 1 Cs-EGTA, 4 MgATP and 10 HEPES (pH 7.3 with CsOH). Spermine tetrahydrochloride or spermidine trihydrochloride (Tocris Bioscience) was added to the intracellular solution as indicated. Rapid solution switching was achieved by piezoelectric translation of a theta-barrel application tool[47] (see Supplementary Methods).

Kinetics of spermine block

The rate of onset of spermine block was studied by using a series of voltage steps from a holding potential of −80 mV to more depolarized potentials (−60 to +80 mV, 20 mV increments, 5 ms duration). The rates of recovery from block were measured in patches held at +20 mV for 15 ms, stepping to a range of more negative potentials (+20 to −80 mV, −20 mV increments). Leak and capacitive currents for each voltage were measured and subtracted. We added 30 μM spermine to the internal solution. Analysis of current waveforms and curve fitting was performed with IGOR Pro 5.05 (Wavemetrics) using NeuroMatic (http://www.neuromatic.thinkrandom.com). Averaged currents describing recovery from block at different potentials were fitted with a double-exponential function:

$$I = A_f \exp(t/\tau_f) + A_s \exp(t/\tau_s) \quad (1)$$

where A_f and τ_f are the amplitude and time constant of the fast component of recovery and A_s and τ_s are the amplitude and time constant of the slow component. If the calculated τ_s was longer than 1s or within 10% of τ_f, a single exponential was used. For double-exponential fits, the weighted time constant of recovery (τ_w) was calculated according to:

$$\tau_w = \tau_f \left(\frac{A_f}{A_f + A_s} \right) + \tau_s \left(\frac{A_s}{A_f + A_s} \right) \quad (2)$$

Measurement of Ca^{2+} permeability

Voltage ramps from −80 to +60mV were applied in control and high-Ca^{2+} (in mM: 30 $CaCl_2$, 110 *N*-methyl-D-glucamine, 5 HEPES and 50 sucrose; pH 7.3 with HCl) solutions, and in the same solutions containing 1mM glutamate and 50μM cyclothiazide. The internal solution did not contain spermine; thus, the maximum current was obtained at all potentials (limited rectification may be ascribed to residual endogenous polyamines). Data obtained were then subtracted for leak and capacitative currents. The relative Ca^{2+} permeability, P_{Ca}/P_{Na}, was determined from the reversal potentials in low-Ca^{2+} extracellular solution (V_{revNa}) and the reversal in high-Ca^{2+} extracellular solution (V_{revCa}) by using the equation:

$$P_{Ca}/P_{Na} = \frac{a_{Na}}{4a_{Ca}} \left(\exp \frac{(2V_{revCa} - V_{revNa})F}{RT} + \exp \frac{(V_{revCa} - V_{revNa})F}{RT} \right) \quad (3)$$

where a_{Na} and a_{Ca} represent the activities of Na^+ and Ca^{2+} in the extracellular solutions (0.87 and 0.64, respectively), and *R*, *T*, and *F* have their conventional meanings2. V_{revNa} and V_{revCa} values were corrected for liquid junction potentials of 4.8 mV (calculated with Clampex 7.1, Molecular Devices Corporation).

NSFA

To deduce channel properties from macroscopic responses, glutamate (10 mM) was applied to outside-out patches (100-ms duration, 1 Hz) and the ensemble variance of all successive pairs of current responses was calculated. The single-channel current (*i*), total number of channels (*N*) and maximum open probability ($P_{o,max}$) were then determined by plotting this ensemble variance (σ^2) against mean current ($\bar{I}$) and fitting with a parabolic function:

$$\sigma^2 = i\bar{I} - \bar{I}^2/N + \sigma^2_B \quad (4)$$

where σ^2_B is the background variance48. Along with expected peak-to-peak variation in the currents due to stochastic channel gating, some patches showed gradual changes in peak amplitude. The mean response was calculated from epochs containing 20–200 stable responses, which were identified by using a Spearman rank-order correlation test (NeuroMatic). The weighted-mean single-channel conductance was calculated from the single-channel current and the holding potential (corrected for the calculated liquid-junction potential; see above). $P_{o,max}$ was estimated by dividing the average peak current by *iN*.

Cerebellar slices

Coronal slices (200 μm) were cut from the cerebellar vermis of P8 (aged 7-8 d), P18 (17-19 d) and P28 Sprague-Dawley rats, in accordance with UK Animals (Scientific Procedures) Act 1986, as described49. Whole-cell recordings were made from visually identified interneurons in the outer third of the molecular layer (presumptive stellate cells) by using standard procedures (see Supplementary Methods). The extracellular solution contained in mM: 125 NaCl, 2.5 KCl, 2 $CaCl_2$, 1 $MgCl_2$, 25 $NaHCO_3$, 1.25 NaH_2PO_4 and 25 glucose (bubbled with 95% O_2 and 5% CO_2). To block NMDA and $GABA_A$ receptors, 20 μM D-AP5 and 20 μM bicuculline methobromide (Sigma) were added. The 'internal' solution contained (in mM): 128 CsCl, 10 HEPES, 10 EGTA, 10 TEACl, 1 QX314 (Tocris), 2 MgATP, 1 $CaCl_2$, 2 NaCl, 0.25 D600 (Sigma) and 0.1 spermine (pH 7.4 with CsOH, final osmolarity 285 ± 5 mOsmol/l). EPSCs were evoked by parallel fiber stimulation using a

Europe PMC Funders Author Manuscripts

patch electrode filled with external solution placed in the molecular layer. Pulses of 60-99 V were applied for 20-200 μs at 0.5 Hz.

EPSC I-V analysis

Evoked EPSCs were filtered at 2 kHz and digitized at 20 kHz. Events without a monotonic rise were rejected. Averages waveforms at each holding potential were generated after aligning a minimum of 20 events at their 20% rise (NeuroMatic, IGOR Pro). Mean EPSC amplitudes were plotted against membrane potential and fitted with a third-order polynomial. The rectification index was calculated by dividing the positive current at +40mV by the negative current value obtained at the membrane voltage equidistant from the reversal potential.

psNSFA

psNSFA was used to estimate the weighted mean single-channel conductance of synaptic receptors39. Spontaneous EPSCs were recorded at −60 mV and detected with a scaled template algorithm50 or by threshold crossing (EVAN software) only events with a fast monotonic rise time and uncontaminated decay were selected for analysis. EPSCs were aligned and averaged. The current was divided into 30 bins of equal amplitude and, within each bin, the variance of the EPSC about the scaled average was computed. The variance was plotted against the mean current value, and the weighted mean single-channel current was estimated by fitting the full parabolic relationship with the equation:

$$\sigma^2_{PS} = i\,\bar{I} - \bar{I}^{\,2}/N_p + \sigma^2_B \quad (5)$$

where σ^2_{PS} is the peak-scaled variance, $\bar{I}$ is the mean current, i is the weighted mean single-channel current, N_p is the number of channels open at the peak of the EPSC, and σ^2_B is the background variance. The mean chord conductance for each cell was calculated by using the reversal potential for that cell.

Statistical analysis

Statistical analysis was performed using PRISM (GraphPad Software), with one- or two-tailed Student's *t*-tests (as appropriate), a Mann-Whitney *U*-test (when data were non-normally distributed; Shapiro-Wilk normality test) or two-way repeated measures of variance (ANOVA).

Free polyamine concentrations

Free spermine concentrations were calculated by using published affinity coefficients for the binding of spermine by ATP and MgATP (see Supplementary Methods). Added concentrations were 1, 3, 10, 30, 100, 300 and 500 μM, giving free concentrations of 0.159, 0.476, 1.59, 4.79, 16.2, 50.5 and 87.5 μM. For 100 μM added spermidine, a free concentration of 31.3 μM was calculated.

Supplementary Material

Refer to Web version on PubMed Central for supplementary material.

Acknowledgments

This work was supported by a Wellcome Trust Programme Grant (SGC-C and MF) and the Royal Society. LK was supported by a Wellcome Trust Studentship during part of this work, and SGC-C holds a Royal Society-Wolfson Research Award. We thank Beverley Clark for valuable help and Roger Nicoll (UCSF) for generously providing TARP DNAs.

Europe PMC Funders Author Manuscripts

References

1. Seeburg PH, Hartner J. Regulation of ion channel/neurotransmitter receptor function by RNA editing. Curr Opin Neurobiol. 2003; 13:279–283. [PubMed: 12850211]
2. Geiger JR, et al. Relative abundance of subunit mRNAs determines gating and Ca^{2+} permeability of AMPA receptors in principal neurons and interneurons in rat CNS. Neuron. 1995; 15:193–204. [PubMed: 7619522]
3. Swanson GT, Kamboj SK, Cull-Candy SG. Single-channel properties of recombinant AMPA receptors depend on RNA editing, splice variation, and subunit composition. J Neurosci. 1997; 17:58–69. [PubMed: 8987736]
4. Feldmeyer D, et al. Neurological dysfunctions in mice expressing different levels of the Q/R site-unedited AMPAR subunit GluR-B. Nat Neurosci. 1999; 2:57–64. [PubMed: 10195181]
5. Bowie D, Mayer ML. Inward rectification of both AMPA and kainate subtype glutamate receptors generated by polyamine-mediated ion channel block. Neuron. 1995; 15:453–462. [PubMed: 7646897]
6. Kamboj SK, Swanson GT, Cull-Candy SG. Intracellular spermine confers rectification on rat calcium-permeable AMPA and kainate receptors. J Physiol. 1995; 486:297–303. [PubMed: 7473197]
7. Koh DS, Burnashev N, Jonas P. Block of native Ca^{2+}-permeable AMPA receptors in rat brain by intracellular polyamines generates double rectification. J Physiol. 1995; 486:305–312. [PubMed: 7473198]
8. Bowie D, Lange GD, Mayer ML. Activity-dependent modulation of glutamate receptors by polyamines. J Neurosci. 1998; 18:8175–8185. [PubMed: 9763464]
9. Rozov A, Burnashev N. Polyamine-dependent facilitation of postsynaptic AMPA receptors counteracts paired-pulse depression. Nature. 1999; 401:594–598. [PubMed: 10524627]
10. Plant K, et al. Transient incorporation of native GluR2-lacking AMPA receptors during hippocampal long-term potentiation. Nat Neurosci. 2006; 9:602–604. [PubMed: 16582904]
11. Adesnik H, Nicoll RA. Conservation of glutamate receptor 2-containing AMPA receptors during long-term potentiation. J Neurosci. 2007; 27:4598–4602. [PubMed: 17460072]
12. Colbourne F, Grooms SY, Zukin RS, Buchan AM, Bennett MV. Hypothermia rescues hippocampal CA1 neurons and attenuates down-regulation of the AMPA receptor GluR2 subunit after forebrain ischemia. Proc Natl Acad Sci U S A. 2003; 100:2906–2910. [PubMed: 12606709]
13. Kawahara Y, et al. Glutamate receptors: RNA editing and death of motor neurons. Nature. 2004; 427:801. [PubMed: 14985749]
14. Kwak S, Weiss JH. Calcium-permeable AMPA channels in neurodegenerative disease and ischemia. Curr Opin Neurobiol. 2006; 16:281–287. [PubMed: 16698262]
15. Cull-Candy S, Kelly L, Farrant M. Regulation of Ca^{2+}-permeable AMPA receptors: synaptic plasticity and beyond. Curr Opin Neurobiol. 2006; 16:288–297. [PubMed: 16713244]
16. Liu SQ, Cull-Candy SG. Synaptic activity at calcium-permeable AMPA receptors induces a switch in receptor subtype. Nature. 2000; 405:454–458. [PubMed: 10839540]
17. Lei S, McBain CJ. Distinct NMDA receptors provide differential modes of transmission at mossy fiber-interneuron synapses. Neuron. 2002; 33:921–933. [PubMed: 11906698]
18. Gardner SM, et al. Calcium-permeable AMPA receptor plasticity is mediated by subunit-specific interactions with PICK1 and NSF. Neuron. 2005; 45:903–915. [PubMed: 15797551]
19. Bellone C, Luscher C. Cocaine triggered AMPA receptor redistribution is reversed in vivo by mGluR-dependent long-term depression. Nat Neurosci. 2006; 9:636–641. [PubMed: 16582902]
20. Chen L, et al. Stargazin regulates synaptic targeting of AMPA receptors by two distinct mechanisms. Nature. 2000; 408:936–943. [PubMed: 11140673]
21. Nicoll RA, Tomita S, Bredt DS. Auxiliary subunits assist AMPA-type glutamate receptors. Science. 2006; 311:1253–1256. [PubMed: 16513974]
22. Ziff EB. TARPs and the AMPA receptor trafficking paradox. Neuron. 2007; 53:627–633. [PubMed: 17329203]

23. Bats C, Groc L, Choquet D. The interaction between Stargazin and PSD-95 regulates AMPA receptor surface trafficking. Neuron. 2007; 53:719–734. [PubMed: 17329211]
24. Tomita S, Fukata M, Nicoll RA, Bredt DS. Dynamic interaction of stargazin-like TARPs with cycling AMPA receptors at synapses. Science. 2004; 303:1508–1511. [PubMed: 15001777]
25. Priel A, et al. Stargazin reduces desensitization and slows deactivation of the AMPA-type glutamate receptors. J Neurosci. 2005; 25:2682–2686. [PubMed: 15758178]
26. Tomita S, et al. Stargazin modulates AMPA receptor gating and trafficking by distinct domains. Nature. 2005; 435:1052–1058. [PubMed: 15858532]
27. Turetsky D, Garringer E, Patneau DK. Stargazin modulates native AMPA receptor functional properties by two distinct mechanisms. J Neurosci. 2005; 25:7438–7448. [PubMed: 16093395]
28. Bedoukian MA, Weeks AM, Partin KM. Different domains of the AMPA receptor direct stargazin-mediated trafficking and stargazin-mediated modulation of kinetics. J Biol Chem. 2006; 281:23908–23921. [PubMed: 16793768]
29. Kott S, Werner M, Korber C, Hollmann M. Electrophysiological properties of AMPA receptors are differentially modulated depending on the associated member of the TARP family. J Neurosci. 2007; 27:3780–3789. [PubMed: 17409242]
30. Yamazaki M, et al. A novel action of stargazin as an enhancer of AMPA receptor activity. Neurosci Res. 2004; 50:369–374. [PubMed: 15567474]
31. Liu SJ, Cull-Candy SG. Subunit interaction with PICK and GRIP controls Ca^{2+} permeability of AMPARs at cerebellar synapses. Nat Neurosci. 2005; 8:768–775. [PubMed: 15895086]
32. Sharp AH, et al. Biochemical and anatomical evidence for specialized voltage-dependent calcium channel gamma isoform expression in the epileptic and ataxic mouse, stargazer. Neuroscience. 2001; 105:599–617. [PubMed: 11516827]
33. Tomita S, et al. Functional studies and distribution define a family of transmembrane AMPA receptor regulatory proteins. J Cell Biol. 2003; 161:805–816. [PubMed: 12771129]
34. Moss FJ, Dolphin AC, Clare JJ. Human neuronal stargazin-like proteins, γ2, γ3 and γ4; an investigation of their specific localization in human brain and their influence on $Ca_V2.1$ voltage-dependent calcium channels expressed in Xenopus oocytes. BMC Neurosci. 2003; 4:23. [PubMed: 14505496]
35. Cu C, Bahring R, Mayer ML. The role of hydrophobic interactions in binding of polyamines to non NMDA receptor ion channels. Neuropharmacology. 1998; 37:1381–1391. [PubMed: 9849673]
36. Rozov A, Zilberter Y, Wollmuth LP, Burnashev N. Facilitation of currents through rat Ca^{2+}-permeable AMPA receptor channels by activity-dependent relief from polyamine block. J Physiol. 1998; 511:361–377. [PubMed: 9706016]
37. Keinanen K, et al. A family of AMPA-selective glutamate receptors. Science. 1990; 249:556–560. [PubMed: 2166337]
38. Petralia RS, Wang YX, Mayat E, Wenthold RJ. Glutamate receptor subunit 2-selective antibody shows a differential distribution of calcium-impermeable AMPA receptors among populations of neurons. J Comp Neurol. 1997; 385:456–476. [PubMed: 9300771]
39. Traynelis SF, Silver RA, Cull-Candy SG. Estimated conductance of glutamate receptor channels activated during EPSCs at the cerebellar mossy fiber-granule cell synapse. Neuron. 1993; 11:279–289. [PubMed: 7688973]
40. Soler-Llavina GJ, Sabatini BL. Synapse-specific plasticity and compartmentalized signaling in cerebellar stellate cells. Nat Neurosci. 2006; 9:798–806. [PubMed: 16680164]
41. Beierlein M, Regehr WG. Local interneurons regulate synaptic strength by retrograde release of endocannabinoids. J Neurosci. 2006; 26:9935–9943. [PubMed: 17005857]
42. Shin J, Shen F, Huguenard JR. Polyamines modulate AMPA receptor-dependent synaptic responses in immature layer v pyramidal neurons. J Neurophysiol. 2005; 93:2634–2643. [PubMed: 15574796]
43. Aizenman CD, Munoz-Elias G, Cline HT. Visually driven modulation of glutamatergic synaptic transmission is mediated by the regulation of intracellular polyamines. Neuron. 2002; 34:623–634. [PubMed: 12062045]
44. Jonas P. The time course of signaling at central glutamatergic synapses. News Physiol Sci. 2000; 15:83–89. [PubMed: 11390884]

45. Lawrence JJ, McBain CJ. Interneuron diversity series: containing the detonation-feedforward inhibition in the CA3 hippocampus. Trends Neurosci. 2003; 26:631–640. [PubMed: 14585604]
46. Bischofberger J, Jonas P. TwoB or not twoB: differential transmission at glutamatergic mossy fiber-interneuron synapses in the hippocampus. Trends Neurosci. 2002; 25:600–603. [PubMed: 12446120]
47. Colquhoun D, Jonas P, Sakmann B. Action of brief pulses of glutamate on AMPA/kainate receptors in patches from different neurones of rat hippocampal slices. J Physiol. 1992; 458:261–287. [PubMed: 1338788]
48. Sigworth FJ. The variance of sodium current fluctuations at the node of Ranvier. J Physiol. 1980; 307:97–129. [PubMed: 6259340]
49. Clark BA, Cull-Candy SG. Activity-dependent recruitment of extrasynaptic NMDA receptor activation at an AMPA receptor-only synapse. J Neurosci. 2002; 22:4428–4436. [PubMed: 12040050]
50. Clements JD, Bekkers JM. Detection of spontaneous synaptic events with an optimally scaled template. Biophys J. 1997; 73:220–229. [PubMed: 9199786]

Europe PMC Funders Author Manuscripts

Europe PMC Funders Author Manuscripts

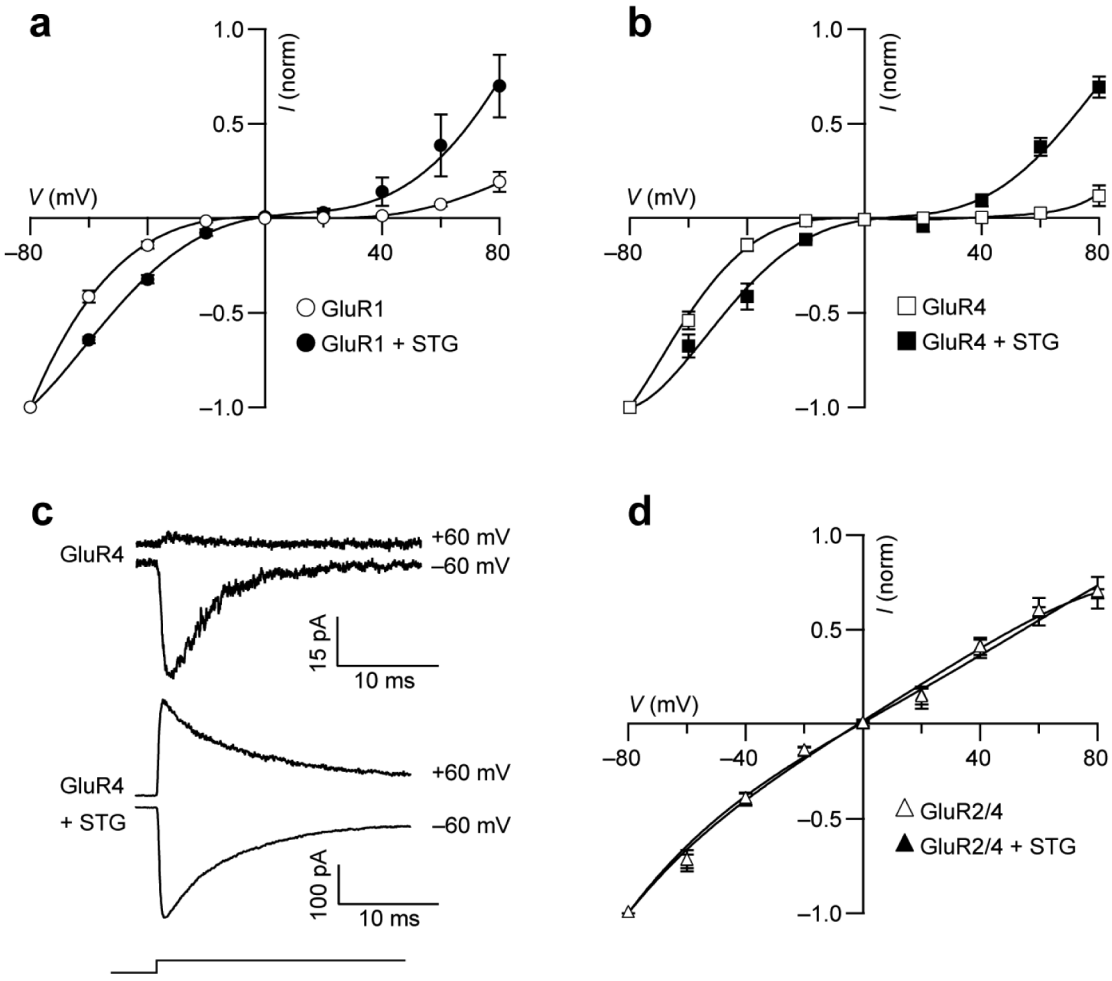

Figure 1.

Stargazin modifies the *I-V* relationship of recombinant Ca^{2+}-permeable AMPAR channels. **(a)** Inwardly rectifying *I-V* relationships for peak currents evoked by glutamate (100 ms, 10 mM) applied to outside-out patches from tsA201 cells containing homomeric GluR1 AMPARs alone ($n = 5$) or with stargazin (STG; $n = 5$). The intracellular solution contained 100 μM added spermine. In all panels, currents are normalized to −80 mV values, error bars denote s.e.m. and lines are fits of fifth- to seventh-order polynomials. **(b)** *I-V* relationships for homomeric GluR4 AMPARs in the same conditions as in ***a***. Subunits were expressed alone ($n = 4$) or with stargazin ($n = 4$). **(c)** Representative glutamate-evoked currents at +60 and −60 mV for Ca^{2+}-permeable homomeric GluR4-containing AMPARs in the absence or presence of stargazin. Step denotes timing and duration of glutamate application. **(d)** *I-V* relationships for cells expressing Ca^{2+}-impermeable AMPARs formed from GluR2 and GluR4 subunits. The *I-V* relationships do not exhibit inward rectification in either the absence ($n = 9$) or the presence ($n = 9$) of stargazin.

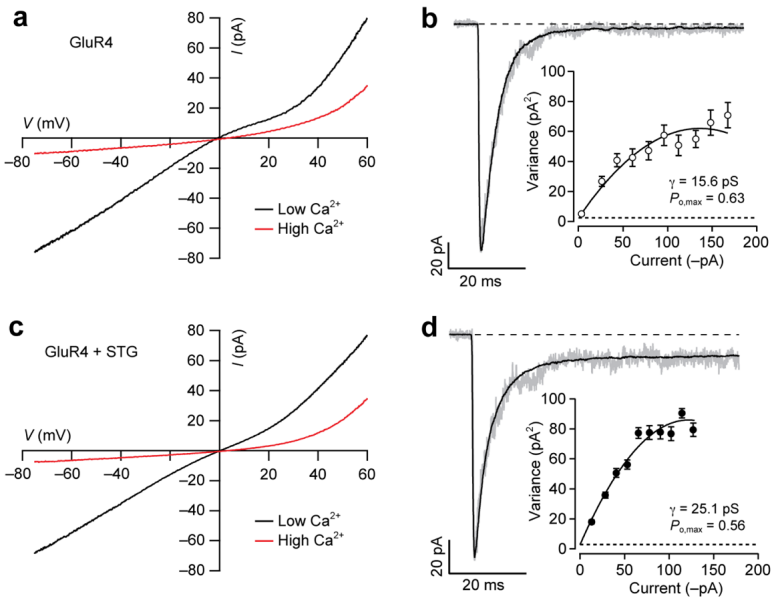

Figure 2.

Stargazin alters conductance but not Ca^{2+} permeability of AMPARs. **(a)** *I-V* relationship for homomeric GluR4 AMPARs. Plots were obtained by ramping membrane potential (duration 1.4s) from −80 to +60 mV in the presence of 1mM glutamate plus 50 μM cyclothiazide. $[Ca^{2+}]_o$ was changed from 1 mM ('low-Ca^{2+}'; $n = 4$) to 30 mM ('high-Ca^{2+}'; $n = 4$). No spermine was added to the pipette solution. The reversal potentials in the two solutions were not different (−0.7 ± 1.1 mV in low Ca^{2+} versus 3.7 ± 0.9 mV in high Ca^{2+}; $n = 4$; P=0.403). **(b)** Currents evoked at −60 mV by rapid application of 10 mM glutamate (100 ms) to outside-out patches from cells expressing homomeric GluR4 AMPARs. Black lines shows mean of 84 traces; gray line showns a representative trace. Inset shows current-variance relationship, the slope of which gave a weighted mean conductance of 15.6 pS for this cell. Broken line denotes the baseline variance. Top data point represents the centre of the bin, so the line stops of calculated maximum ($P_{o,max}$ = 0.63) **(c, d)** As in ***a*** and ***b***, but with GluR4 AMPAR subunits coexpressed with stargazin. The reversal potential was 0.3 ± 0.5 mV at 1 mM $[Ca^{2+}]_o$ and 3.4 ± 0.9 mV at 30 mM $[Ca^{2+}]_o$ (both $n = 5$; P=0.254). A single macroscopic response and the mean of 121 responses is shown in **d**. Inset shows current-variance relationship, yielding a weighted mean conductance of 25.1 pS.

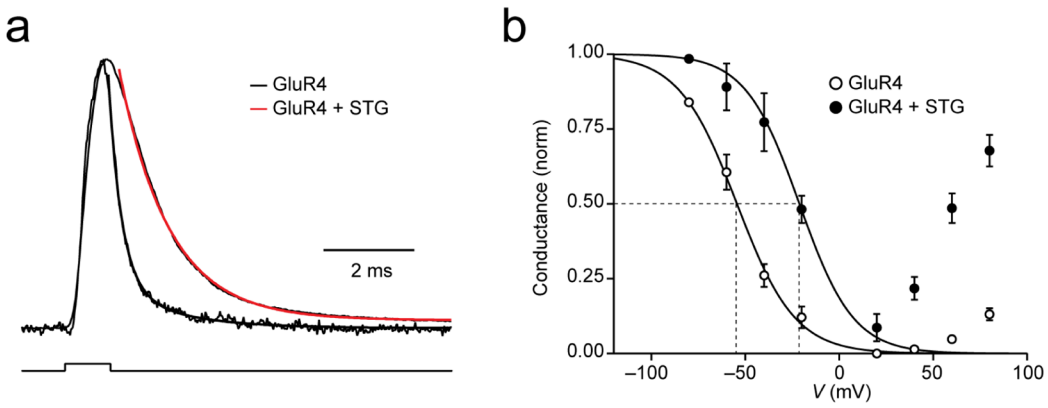

Figure 3.

Effect of stargazin on polyamine block and deactivation of GluR4 AMPARs. **(a)** Representative current responses recorded from outside-out patches containing GluR4 receptors with and without stargazin (step denotes 1 ms application of 1 mM glutamate; −60 mV with 100 μM added spermine). Responses are scaled to the same peak amplitude and their decays fitted with double exponentials: GluR4, τ_f = 0.40 ± 0.05 ms (71 ± 9.3%), τ_s = 1.6 ± 0.5 ms; GluR4 plus stargazin, τ_f = 1.41 ± 0.33 ms (89.9 ± 3.4%) τ_s = 16.4 ± 7.1 ms (both n=4). τ_w increased from 0.61 ± 0.14 to 2.52 ± 0.64 ms (P=0.0271), and the normalised charge transfer increased from 1.00 ± 0.13 to 2.41 ± 0.42 ms (+141%; P=0.0146). **(b)** Plot of normalized conductance (G) against voltage (V_m) for GluR4 receptors with and without stargazin (data from Fig. 1b). Unbroken lines are fits (at negative voltages) to a Boltzmann function:

$$G=G_{max}\left(\frac{1}{1+\exp\left((V_m - V_{1/2})/k\right)}\right),$$

where G_{max} is the maximal glutamate-activated conductance at hyperpolarized voltages, $V_{½}$ is the voltage at which spermine block is half-maximal (broken lines) and k is a slope factor describing the membrane potential shift necessary to cause an e-fold change in conductance. The slopes of the fits were not different (k = 15.5 mV for GluR4 and 14.4 mV for GluR4 plus stargazin) but $V_{½}$ shifted from −54.4 to −21.2 mV. Similar results were obtained with GluR1).

Europe PMC Funders Author Manuscripts

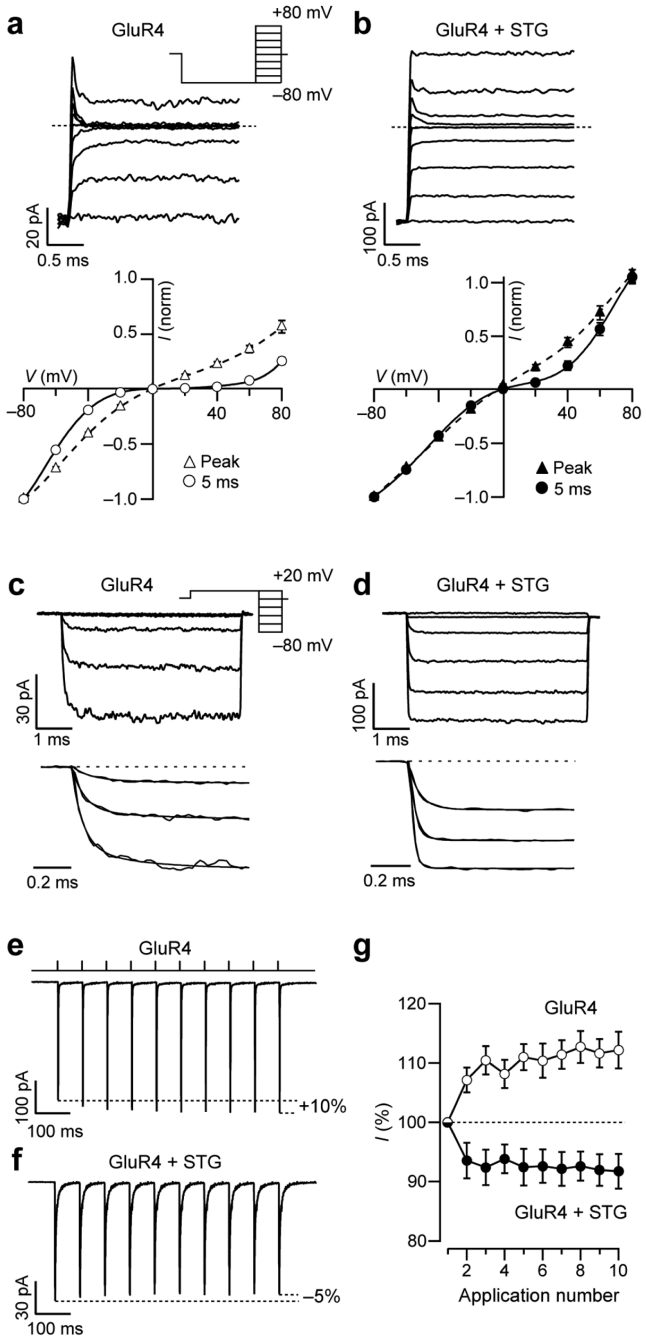

Figure 4.

Stargazin alters the time course of spermine block and eliminates frequency-dependent facilitation of Ca^{2+}-permeable GluR4 AMPARs. **(a, b)** Top, representative responses of homomeric GluR4 AMPARs, alone (**a**) or with stargazin (**b**), to depolarizing voltage steps in the presence of 1 mM glutamate. After a hyperpolarizing pre-pulse to −80 mV, outside-out patches were stepped to +80 mV in 20 mV increments (inset). Cyclothiazide (50 μM) was included in the extracellular medium to minimize desensitization, and the 'intracellular' solution contained spermine (30 μM). Broken line indicates zero current. Relaxations following voltage steps were greatly diminished with stargazin. Bottom, corresponding *I-V*

relationships for peak and steady-state (5 ms) currents (n = 7 cells without and n = 5 cells with stargazin). **(c, d)** Top, relaxation responses to hyperpolarizing voltage steps in the presence of 1mM glutamate applied to patches containing GluR4 (**c**) or GluR4 plus stargazin (**d**). The potential was stepped from +20 mV to −80 mV in −20 mV increments (after a pre-pulse from 0 to +20 mV; inset). Cyclothiazide and spermine were included as in **a,b**. Bottom, onset of the currents; those recorded at −80 to −40 mV were fitted with exponentials. The kinetics of the currents following voltage steps was much faster in the presence of stargazin. **(e, f)** Currents activated by a train of glutamate pulses (1 mM, 1 ms) applied at 14 Hz to patches expressing GluR4 (**e**) or GluR4 plus stargazin (**f**). Currents from GluR4 alone increased in amplitude during the train, whereas those from GluR4 plus stargazin showed depression (−60 mV; 10 μM intracellular spermine). Traces are averages of 60 or 100 trials. **(g)** Pooled data from cells expressing GluR4 alone ($n = 16$) or GluR4 with stargazin ($n = 9$; $P < 0.0001$ by two-way repeated measures ANOVA).

Europe PMC Funders Author Manuscripts

Europe PMC Funders Author Manuscripts

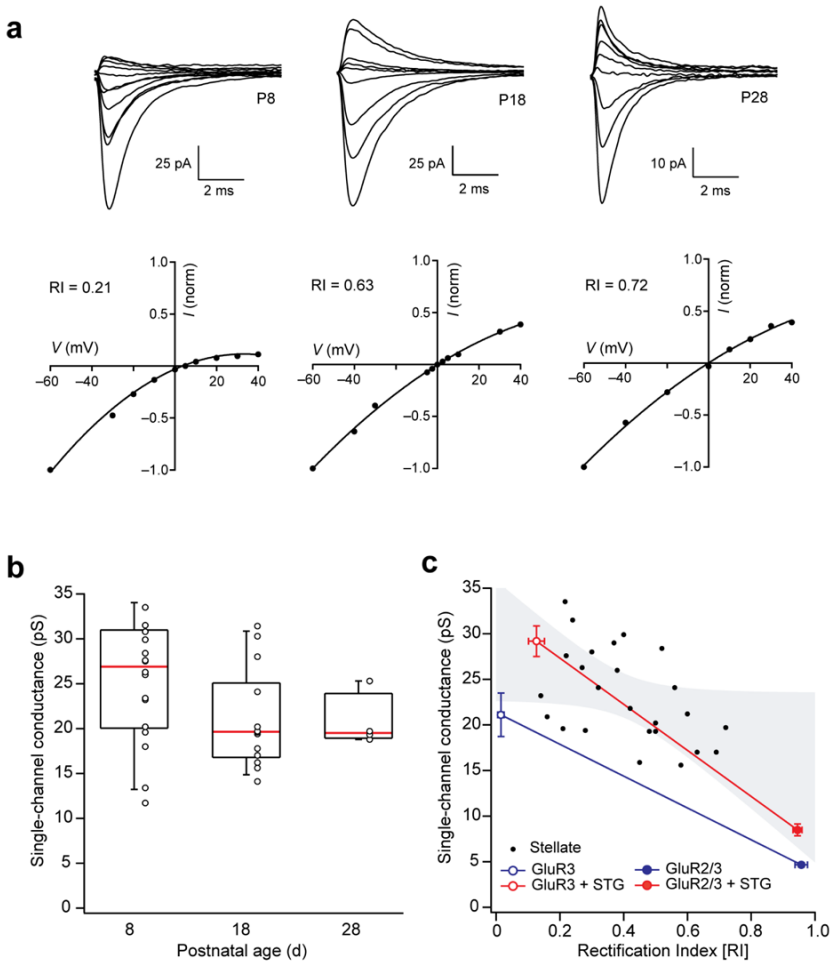

Figure 5.

Rectification and conductance properties of synaptic AMPARs are consistent with the presence of stargazin. **(a)** Top, representative stellate cell EPSCs evoked by parallel fiber stimulation at three different ages (P8, 18 and 28). Bottom, corresponding peak *I-V* relationship. RI denotes the rectification index (**Methods)**. (**b**) Plot of single-channel conductance for AMPARs determined from spontaneous EPSCs at three different ages. Values from individual cells are shown with box-and-whisker plots (indicating median, 25-75th and 10-90th percentiles). (**c**) Scatter plot of rectification index for stellate cell-evoked EPSCs against single-channel conductance determined from psNSFA of spontaneous EPSCs in the same cells. Filled circles represent individual cells; gray shading indicates the 99% confidence limits of a linear fit to the data ($n = 23$; P=0.023 by Spearman rank-order correlation; fit removed for clarity). Superimposed on this graph are corresponding data from two sets of recombinant receptors (GluR3 and GluR2/GluR3) with and without stargazin. Symbols indicate mean, and vertical and horizontal error bars denote s.e.m. for each condition. Note that only receptors with stargazin mimic the properties of the synaptic receptors.

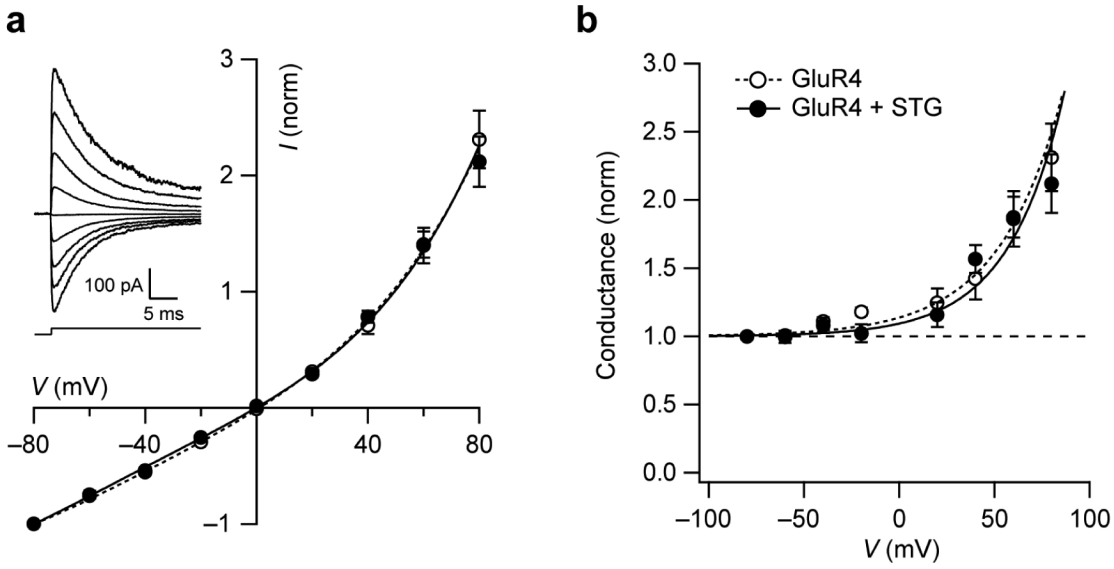

Figure 6.

Stargazin does not affect rectification of GluR4 in the absence of polyamines. **(a)** *I-V* relationships for homomeric GluR4 receptors with and without stargazin in the absence of spermine. Na_2ATP (20 mM) was included in the patch pipette to chelate endogenous polyamines. The *I-V* relationships are normalized to the current obtained at −80 mV and show identical outward rectification in the presence and absence of stargazin (n = 5 each; symbols as in **b**). Vertical error bars denote s.e.m. and fitted lines are fifth-order polynomials. Inset shows a family of GluR4 currents (−80 to +80 mV) in response to application of 10 mM glutamate (indicated by the step). **(b)** Plots of normalized conductance against voltage for the data shown in **a**. Fitted lines are drawn according to $G = G_{min} + (G_0 - G_{min})\exp(V_m / V_c)$, where G_0 is the conductance at 0 mV, G_{min} is the minimal conductance (normalized value of 1), and V_c is a constant. Without stargazin, G_0 was 1.14 and V_c 33.5 mV. With stargazin, the respective values were 1.09 and 29.4 mV.

Europe PMC Funders Author Manuscripts

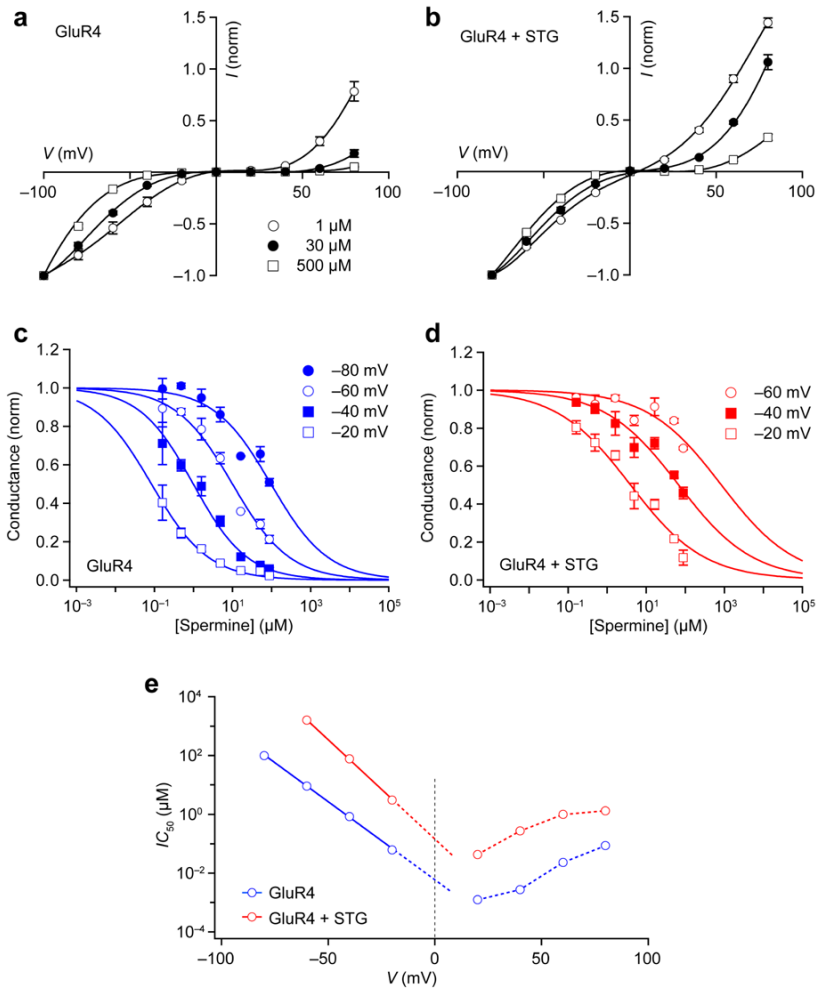

Figure 7.

Stargazin reduces the apparent affinity of GluR4 receptors for spermine. **(a**, **b)** *I-V* relationships for homomeric GluR4 receptors recorded with different concentrations of added intracellular spermine in the absence (**a**) and presence (**b**) of stargazin. *I-V* curves were generated for added spermine concentrations of 1, 3, 10, 30, 100, 300 and 500 μM, but for clarity only three are shown. Currents from individual cells (n = 3–5) are normalised to the response obtained at the largest negative voltage (−100 and −80 mV, respectively). Vertical error bars denote s.e.m. Lines are fits of fifth- to seventh-order polynomials. (**c**, **d**) Plots of normalized conductance at different voltages (derived from data in **a** and **b**). For clarity, only data obtained at negative voltages are shown. Unbroken lines show global fits of each data set (with and without stargazin) to the equation: $G = 1/1+ (IC_{50} /[\text{Spm}])^{n_H}$, where IC_{50} is the concentration of spermine (Spm) producing a half-maximal reduction in the conductance and n_H is the slope factor (Hill coefficient). (**e**) Plot of IC_{50} against membrane voltage. For the data obtained at negative voltages, fitted lines extrapolated to 0 mV (vertical broken line) indicate IC_{50} values at 0 mV of 21 and 460 nM for GluR4 and GluR4 plus stargazin, respectively. Broken lines also connect the IC_{50} values obtained at positive voltages.

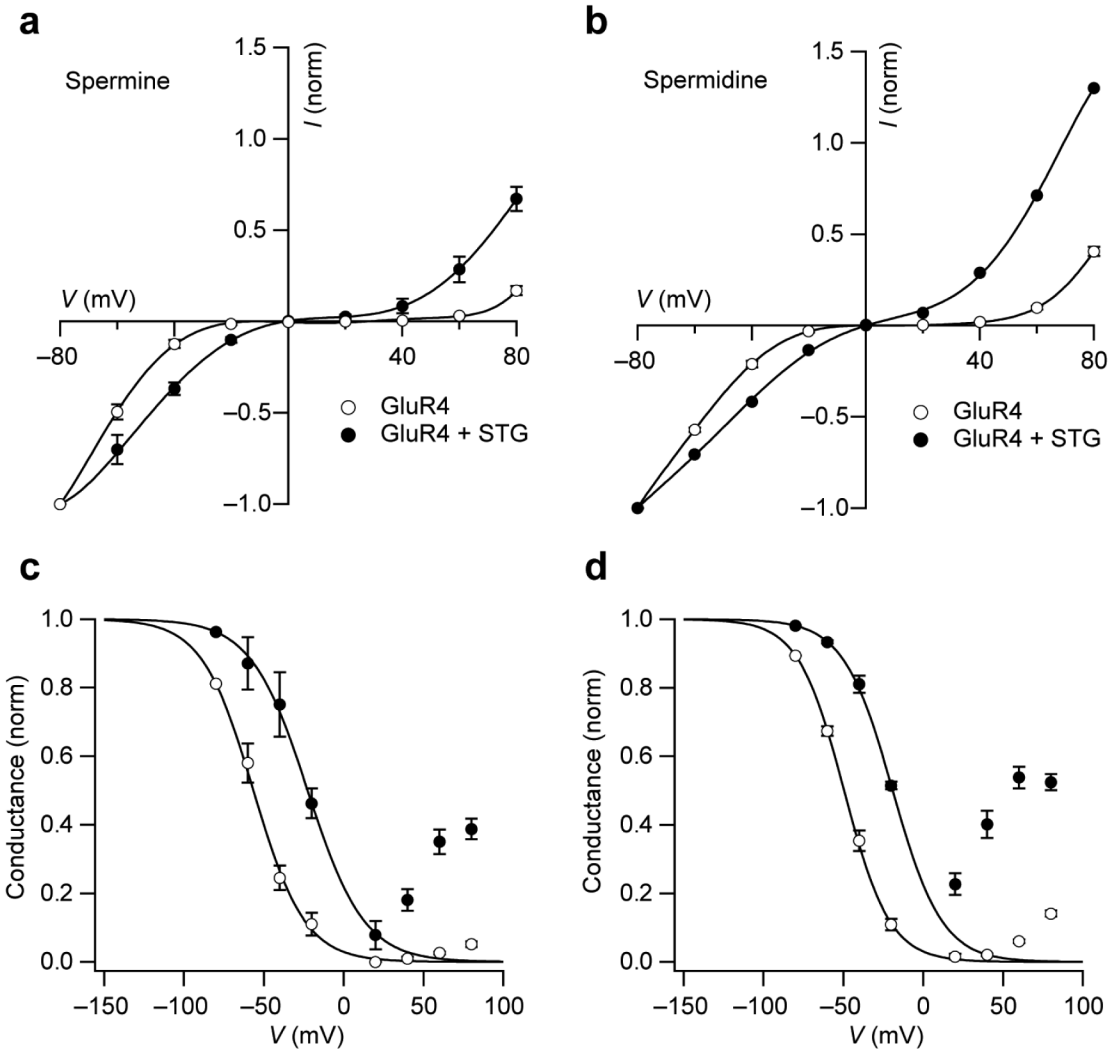

Figure 8.

Stargazin modifies spermidine block of GluR4 receptors. **(**a,**b)** *I-V* relationships for GluR4 receptors obtained with spermine (**a**) or spermidine (**b**) added to the intracellular solution (100 μM). Data were recorded from cells with or without stargazin, as indicated. Currents are normalized to −80 mV values (n = 3 in each condition), error bars denote s.e.m., and lines are fits of fifth- to seventh-order polynomials. (**c d**) Plots of normalized conductance against voltage for the data shown in **a** and **b** (corrected for the outward rectification observed in the absence of polyamines; Fig. 6). Unbroken lines are fits to the data at negative voltages of a Woodhull model for a non-permeable blocker (see text). This fit gave values for $K_{d(0)}$ of 0.49 and 4.54 μM for spermine and 0.98 and 9.1 μM for spermidine in the absence and presence of stargazin, respectively.